Laves phase embrittlement of the ferritic stainless steel type AISI 441

By M.P Sello[1] and W.E Stumpf

Department of Materials Science and Metallurgical Engineering of the University of Pretoria, South Africa with [1] currently at Bhp Billiton, Hillside Aluminium Smelter, Richards Bay, 3900, South Africa.

Corresponding author: maitse_s@hotmail.com; cell: +27 72 514 3047, tel: +27 39 908 9433

Abstract

The effect of Laves phase (Fe_2Nb) formation on the Charpy impact toughness of the ferritic stainless steel type AISI 441 was investigated. The steel exhibited good room temperature toughness after solution treatment of 30 minutes at 850°C, but above and below this treatment temperature the room temperature impact toughness decreased sharply. In as received and already brittle specimens where different volume fractions of Laves phase were introduced through isothermal equilibration at various temperatures below 850°C it was observed that a decrease in the Laves phase volume fraction with increasing annealing temperature towards 850°C (Thermocalc$^{(R)}$ predicted a Laves phase solvus temperature of 825°C versus a later measured solvus of 875°C for this steel) corresponded to an increase in the impact toughness of the steel. On the other hand, annealing at various temperatures above 900°C where no Fe_2Nb exists, grain growth was found to also have a very negative influence on the steel's room temperature impact properties. Through deliberate prior grain growth and by varying the cooling rate after solution treatment, it was found that where both a large grain size and Fe_2Nb are present, it appears that the grain size is the dominant embrittling mechanism. It was possible to qualitatively relate the impact strength results to current models on the effects of grain size and brittle grain boundary precipitates on the brittle fracture of ferritic materials. Finally, both the presence of Fe_2Nb and grain growth, therefore, have a significant influence on the impact properties of the type 441 stainless steels, which necessarily leads to a relatively narrow final hot rolling temperature processing "window" followedby rapid cooling rates in the manufacturing process.

Keywords: Fe_2Nb, titanium niobium carbonitrides (Ti,Nb)(CN), embrittlement, grain size, ductile-to brittle transition temperature (DBTT)

1 Introduction

The automobile industry is currently driven by safety and environmental regulations, specifically the need for drastic reductions in gas emissions. For this, it is necessary to increase the exhaust gas temperature to approximately 900°C and to reduce the weight of the exhaust system [1,2] and the automobile industry is searching for alternative or new materials. These must have excellent heat resistant properties, especially thermal fatigue resistance [3]. Mild steel is, therefore, being replaced by other materials, which have good thermal fatigue resistance and are light in weight.

Materials for this application should have both high yield strength at high temperature and a low coefficient of thermal expansion. Ferritic stainless steels have a relatively low coefficient of thermal expansion and, therefore, some efforts have been made to create new ferritic stainless steels with high yield strengths at elevated temperatures, particularly by the addition of niobium (Nb) which increases the initial high temperature strength through solid solution hardening.

Stainless steel AISI 441 is used in the manufacture of vehicle catalytic converter shells. It is a Ti and Nb dual stabilised ferritic stainless steel with improved stress-corrosion resistance and mechanical properties from solid solution hardening [4-6]. The alloying elements also lead to the formation of a variety of precipitates such as Nb(C,N) and Ti(C,N) (carbo–nitrides), Fe_2Nb (Laves phase) and Fe_3Nb_3C (M_6C carbide). The effect of these Nb precipitates on the high temperature strength of these steels is still being debated, but it has been reported that rapid coarsening of the Laves phase significantly reduced the high temperature strength [6,7]. However, detailed analyses of these effects have not yet been made.

Embrittlement is experienced from time to time during the processing of type AISI 441 steel. This problem is considered to possibly be generic because it appears in the hot band material prior to annealing, whereby the material is found to be brittle after being coiled. It has been suggested that the embrittlement might be from the formation of the intermetallic Fe_2Nb during or after hot rolling combined with slow cooling [8]. After rolling on the hot finishing mill at Columbus Stainless, the finishing temperature of the steel strip is approximately 900°C, and the strip is then rapidly cooled to below 600°C by laminar cooling with water sprays on the run-out table to avoid Fe_2Nb formation and is then coiled. In a few cases hot rolled coils have been found to be brittle and could not be processed further, an embrittlement that was found not to be from any growth in ferrite grain size [8].

Nb additions to these steels improve their high temperature strength by solid solution hardening. However, solute Nb can precipitate as carbo–nitrides and/or Fe_2Nb if the steel is processed or used at high temperatures. Fine Fe_2Nb precipitates which formed during the early stages of ageing, contributed to high temperature strength in a 0.01C – 0.38Nb ferritic stainless steel [9], whereas fine Fe_2Nb precipitates, in spite of its large quantity, did not reduce the impact value as much as the coarser Laves phase that had formed on the grain boundaries upon slow cooling. An attempt is made here to obtain a better understanding of the effect of annealing temperature, grain size and cooling rate after solution treatment on the effect that the steel's Laves precipitates have on the impact properties. In a parallel study to be reported elsewhere, the precipitation kinetics of the Laves phase in this and other similar steels, have been quantified through XRD of electrolytically extracted precipitates and a *TTP* diagram for their formation has been established [10].

2 Experimental procedure

Table 1 shows the chemical composition of the AISI 441 steel that was used in this study, which was supplied by Columbus Stainless as a 7.8mm thick hot band material after it was found to be too brittle for further processing. The equilibrium fraction and the dissolution temperature of the various expected precipitates for this composition were calculated using Thermo-Calc® (TCFE3 database) and were compared to quantitative volume fraction measurements by XRD of the Laves and carbo-nitride second phases from electrolytically extracted precipitates from solution treated and isothermally annealed specimens. For impact fracture purposes, as received specimens of the already brittle coil that contained a large volume fraction of secondary phases, were isothermally annealed in the temperature range of 600 – 1100°C for 30 min in an argon atmosphere and then water – quenched to bring the already existing secondary phases to isothermal equilibrium in volume fractions. Both Charpy impact and tensile test specimens were prepared as subsize specimens in accordance with ASTM E23 and ASTM E8, respectively. Both the Charpy and the tensile specimens were machined in a direction transverse to the rolling direction, whereas the notches were machined parallel to the rolling direction but within the rolling plane. All the tests were performed at room temperature, except for those where the ductile-to-brittle transition temperatures (DBTT) were determined.

Table 1. Chemical composition (wt.%) of the type 441 ferritic stainless steel.

C	Cr	Mn	Co	V	Si	Ti	Ni	N	Nb
0.012	17.89	0.51	0.03	0.12	0.5	0.153	0.19	0.0085	0.444

Metallographic specimens were etched electrolytically in a 60% nitric acid solution at a constant potential of 1.5 V dc for a period of 30 to 120 sec. Scanning electron microscopy (SEM) samples were etched for longer periods for secondary phase analysis. A Joel JSM–6300 scanning electron microscope (SEM) was used for EDS analyses of the secondary phases. Quantitative weight fraction determinations from electrolytically extracted precipitates on solution treated and isothermally annealed specimens were carried out by XRD as reported elsewhere [10]

The effect of cooling rate on the embrittlement of this steel was investigated using a Gleeble® 1500D Thermal Simulator by using subsize Charpy samples that were solution annealed in situ at temperatures of 850 and 950°C for 5 min in an inert argon atmosphere followed by programmed forced cooling with helium at different linear cooling rates of between 1 and 50°C/s.

3 Results

3.1 Equilibrium thermodynamic modelling by Thermo-Calc®

The recommended temperature range when using Thermo-Calc® (TCFE3 database) is from 700 to 2000°C [11]but the thermodynamic data for the intermetallic Laves phase within the data base are less reliable than for many other phases within this steel.

Fig.1(a) shows the Thermo-Calc® prediction of equilibrium weight fraction of the Laves phase for this particular composition of steel as a function of annealing temperature, which is estimated to be about 0.62wt.% at 700°C, decreasing gradually until the solvus temperature of 825°C of the Laves phase is reached, which is in broad agreement with general results from others on similar steels [5,6,12]. The XRD analysis of the as-received plant-brittle steel indicate that the weight percentages for the Laves phase and (Ti,Nb)(C,N) to be about 1.14% and 0.33%, respectively. On the same Fig 1 the measured weight fractions for equilibrium annealing are also shown. Note that the measured Laves phase equilibrium solvus temperature appears to be about 875°C against the predicted value of 825°C for this particular steel composition. Thermo-Calc® predicts that the composition of the Laves phase consists mainly of Fe and Nb in the ratio 2:1, with less than 0.1% mole fraction of other alloying elements such as Ti and Cr present. Therefore, it can be concluded that the composition of the Laves phase is most likely a Nb-rich $(Fe,Cr)_2(Nb,Ti)$ and this was confirmed in this steel by both SEM-EDS and TEM-EDS analyses [10]. Fig.1(b) shows an isopleth section for the ternary phase diagram of stainless steel type 441 in which the expected presence of the (Ti,Nb)(C,N) is confirmed. This figure predicts that the stable phases in this steel

with 0.012%C (marked with the arrow in Fig. 1(b)) are the Laves phase, carbo–nitrides and the sigma phase in a structure that remains completely ferritic from its initial solidification.

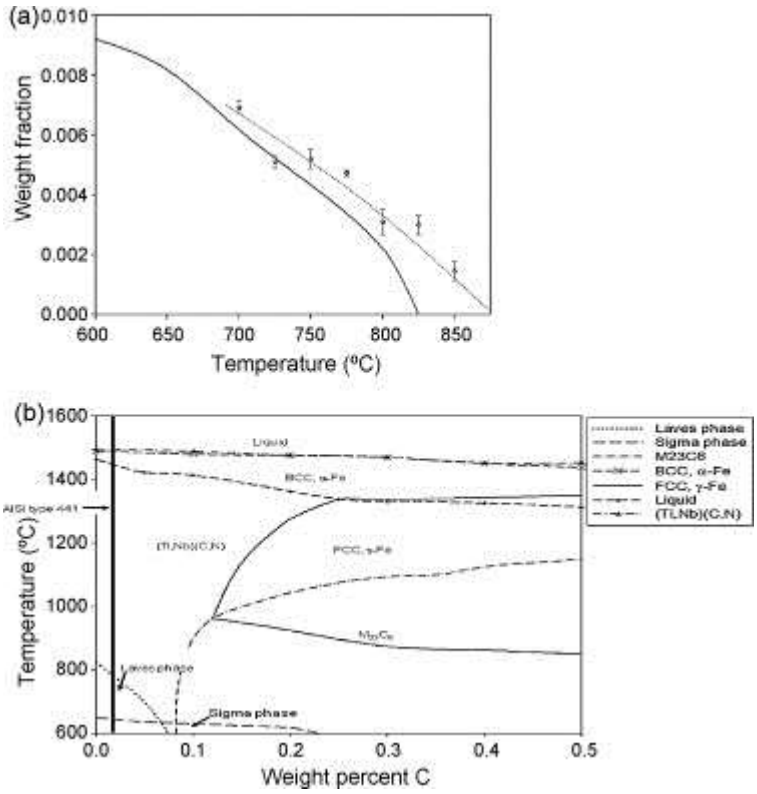

Fig. 1. Thermo-Calc® calculations for the (a) equilibrium weight fraction of Laves phase in this composition of AISI 441 steel. The dotted line and data points lying above the full line, are the actually XRD measured equilibrium weight fractions. (b) The isopleth diagram at 17.9%Cr showing the stable equilibrium phases in type 441 stainless steel with a constant amount of alloying elements and 0–0.5 wt.% of carbon.

3.2 Effect of solution treatment on the microstructural and mechanical properties

The morphology of the various precipitates changes with the annealing treatment, as revealed by the two types of precipitates observed by SEM in Fig. 2. Only the large particles could be analysed successfully while the small precipitates were later analysed using transmission electron microscopy (TEM) and XRD techniques and were found to be the Laves phase.

The SEM results from Fig. 2 confirm the Thermo-Calc® predictions, in that both nitrides and carbides form as complex FCC (Ti,Nb)(C,N) precipitates with the Ti(C,N) nucleating first and then the Nb(C,N) nucleating on its surface as a shell or alternatively as a cluster of loose particles around the Ti(C,N). This is not surprising as Ti(C,N) is known to have a lower solubility than Nb(CN) and will, therefore, form first during cooling from the melt while the Nb(CN) forms at slightly lower temperatures by heterogeneous nucleation on the existing Ti(CN). Craven et al.[13] observed that the (Ti,Nb)(C,N) complex has a least soluble core

consisting of TiN that precipitates at higher temperatures during cooling from the melt, and the Nb/Ti ratio in the core is markedly affected by the cooling rates during solidification and later thermomechanical processing. From the extracted precipitates, the weight percentage of (Ti,Nb)(CN) in the steel after solution treatment and isothermal annealing was measured as only about 0.108% for all annealing temperatures from 600 to 900°C, a value that is confirmed by Thermo-Calc® predictions and is much smaller than the typical measured and predicted Laves phase weight fractions.

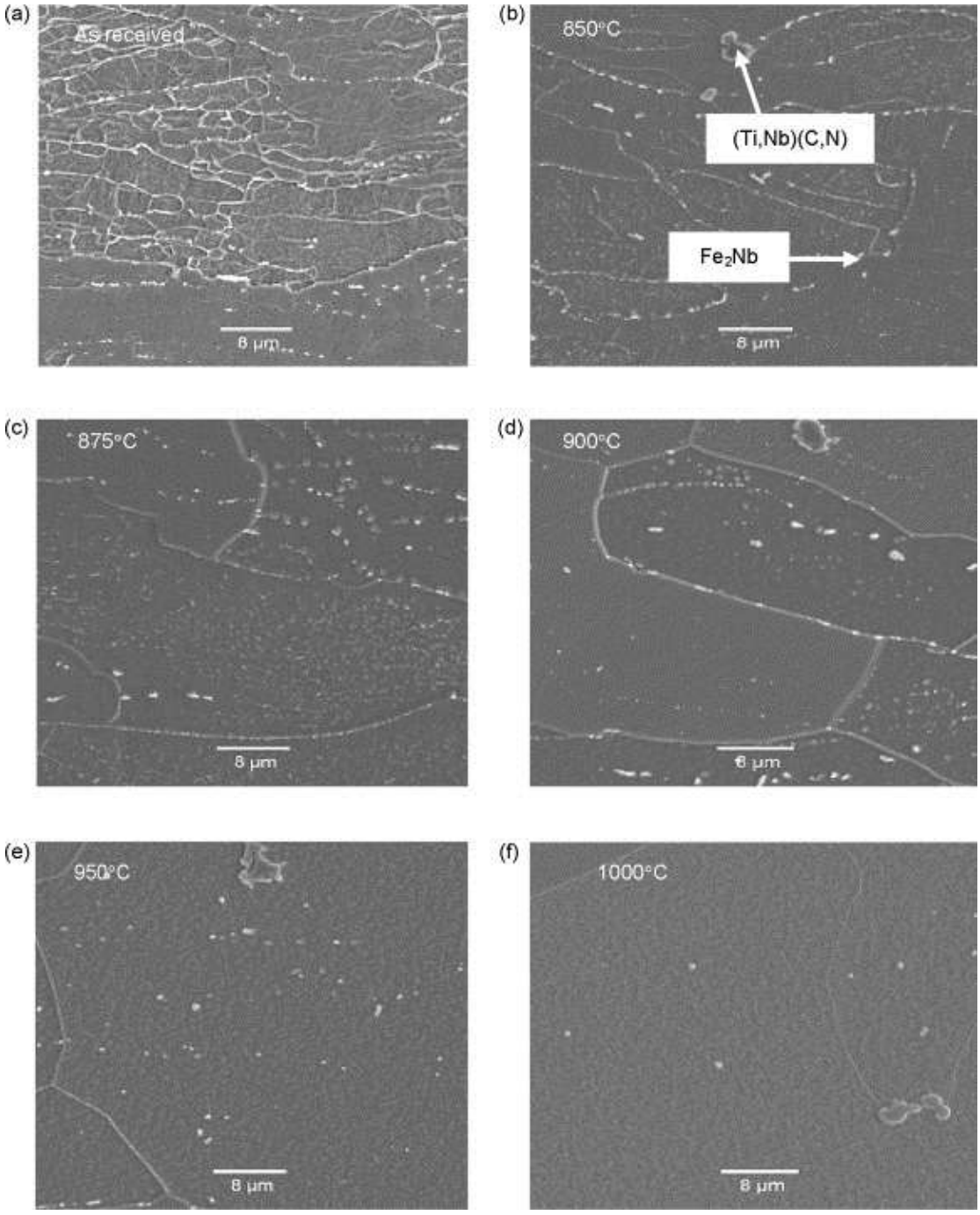

Fig. 2. SEM micrographs showing the effect of annealing temperature on the morphology of the second phase. (a) As received; and solution annealed at: (b) 850 °C; (c) 875 °C; (d) 900 °C; (e) 950 °C; (f) 1000 °C.

The SEM results in Fig. 2 also confirm qualitatively that the volume fraction of fine Laves phase precipitates in the isothermally equilibrated as received specimens as a function of annealing temperature decreases in quantity as the annealing temperature increases in a manner similar to the Thermo-Calc® predictions as well as the measured equilibrium values after solution treatment and isothermal annealing. The decrease in weight fraction as the solvus temperature is approached releases an equivalent amount of niobium into solid solution which will increase the high temperature strength of this material [1,4,5].

The results for the room temperature Charpy impact tests of the as received but equilibrated specimens as a function of isothermal annealing temperature are shown in Fig. 3, with the as received plant-brittle specimens showing an impact strength of only 10J. The Charpy Impact Energy (CIE) of the subsequently equilibrated specimens shows a maximum of about 60J for the specimens annealed at 850°C, but with a decreasing CIE on both sides of this temperature. Annealing at 900°C and above where no Laves phase was found to be present, the CIE averaged only 10J. It is concluded that above 850°C, grain growth plays a major role in lowering the impact energy, but below 850°C where no significant grain growth was found to occur, the precipitation of the intermetallic Laves phase appears to contribute to the lowering of the impact toughness. Comparing these results with both the predicted and measured values from Fig. 1, it is seen that as the volume fraction of the Laves phase decreases with a rise in the annealing temperature towards the predicted solvus of 850°C, the impact toughness also increases to its maximum of 60J. Beyond 850°C the observed grain growth plays a major role in embrittling this steel, a problem that is well known in most ferritic stainless steels.

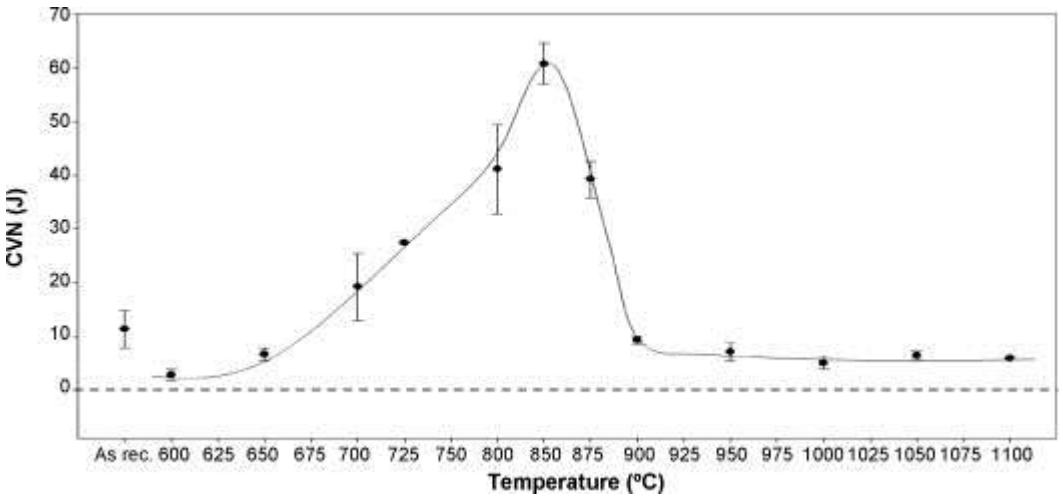

Fig. 3. Effect of annealing temperature on the room temperature Charpy impact energy of the as hot rolled and annealed steel. The specimens were annealed at temperature for 30 min and then water quenched.

Typical fracture surfaces after annealing treatments are shown in Fig. 4. In Fig. 4(a) the plant-brittle material with a CIE of only about 10J is shown, with the fracture surface revealing both macro- and micro-voids in a dimpled surface which is characteristic of a ductile failure although the CIE was relatively low. The particles within the voids in Fig. 4(a) were identified as “blocky” (Ti,Nb)(C,N) precipitates. These macro-voids appear to be formed by the presence of these large cuboidal particles which indicates a low cohesive force between them and the steel matrix. These precipitates which are few in number are, therefore, possibly not the direct cause of the brittleness of the alloy. The presence of the Laves phase on the grain boundaries (see Fig. 4(a)) has, therefore, contributed to the brittleness of the material.

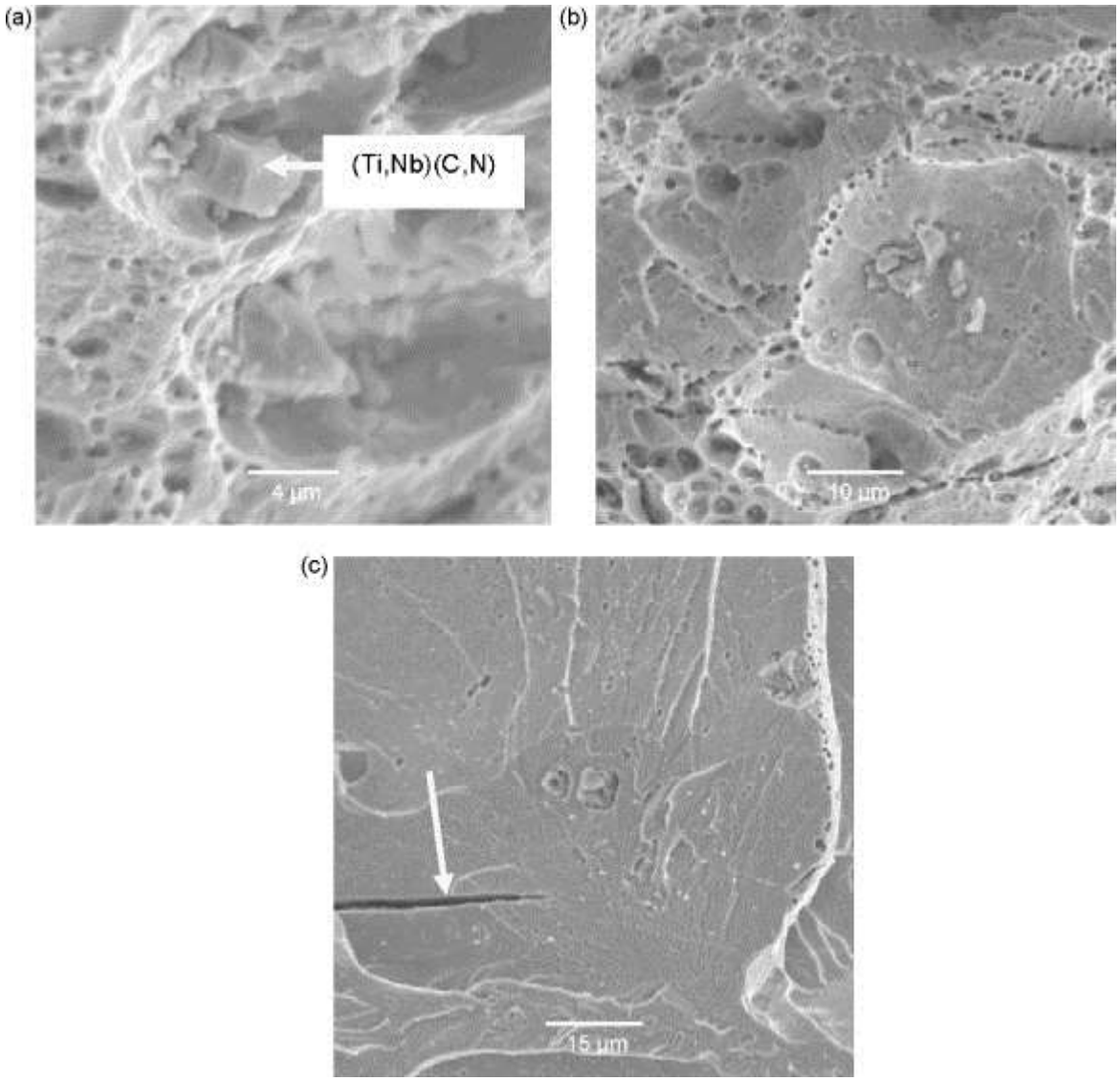

Fig. 4. Examples of the Charpy fracture surfaces after annealing at the temperatures of: (a) as received specimen; (b) annealed at 850 °C; and (c) annealed at 900 °C. Note the arrowed internal cracks.

Fig. 4(b) shows the fractograph of the specimen after annealing at 850°C at the maximum CIE, indicating a ductile fracture. There are no obvious differences in the failure mode between the plant-brittle material with a CIE of only about 10J and the sample annealed at 850°C with a CIE of 60J, except that there are some Fe_2Nb precipitates still present on the grain boundaries (see Fig. 2(b)). Previous studies have shown that the presence of Laves phase degrades the mechanical properties of this high chromium ferritic steel within the temperature range of 500 – 750°C [12]. Fig. 4(c) shows the fracture surface after annealing at 900°C; showing transgranular cleavage with individual grains identified by changes in the river markings. Fig. 4 (c) shows microcracks that are clearly visible on the fracture surface. Some cleavage or grain boundary microcracking was occasionally observed (see arrow in Fig.4(c), but little role of microstructure in crack initiation could be inferred directly.

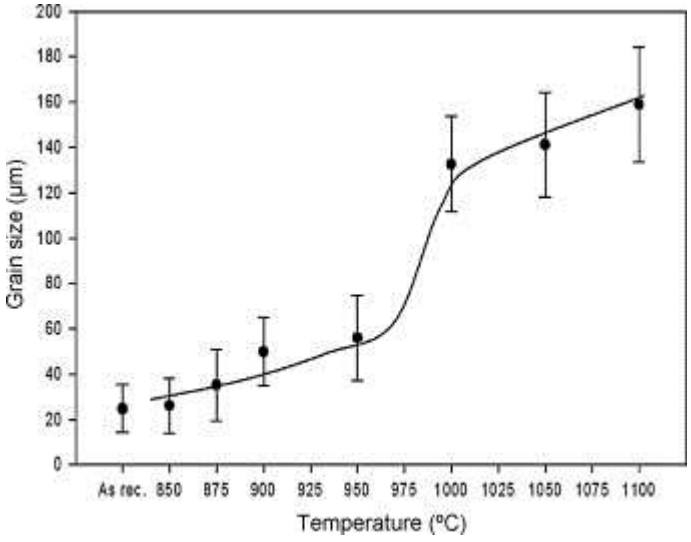

Fig. 5. Effect of annealing temperature above 850 °C on the grain size.

Fig. 5 shows the grain size as a function of the annealing temperature above the predicted solvus of 825°C (and actual 875°C) where grain growth is expected. There is a steady increase in grain size up to about 950°C, but between 950 and 1000°C there is a sudden and rapid 60% increase in grain size. Fig. 6 shows the TEM micrographs after annealing at 850 and 900°C respectively, with some remnants of Laves phase after annealing at 850°C, but at 900°C this phase had completely dissolved. This confirms the observation from Fig. 1 that the true solvus temperatures for the Laves phase in this particular composition of steel lies above 850°C, i.e. at about 875°C and not at the predicted 825°C.

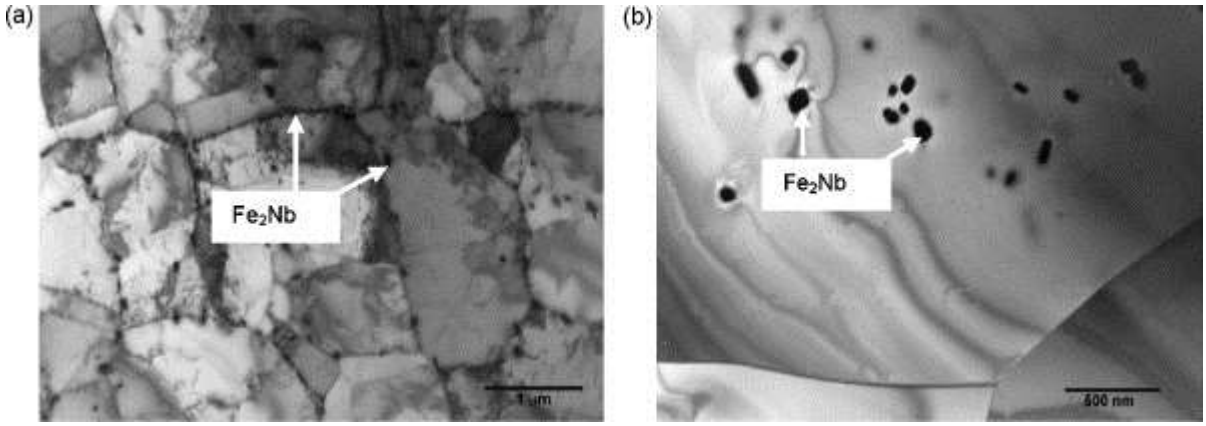

Fig. 6. TEM micrographs of the microstructures of the specimens that were annealed at (a) 850 °C and (b) 900 °C. Note that at 900 °C, there were no grain boundary Laves phase precipitates.

Fig. 7 shows the tensile properties after annealing at and above 850°C. Both the $R_{p(0.2\%)}$ and R_m decrease whilst the elongation increases with increasing annealing temperature. Significantly, however, after annealing at 850°C a relatively poor elongation is found whereas at 900°C the elongation had increased significantly, indicating that at 850°C some last embrittling Laves phase was still present while at 900°C it had completely dissolved. The effect of grain growth on the $R_{p(0.2\%)}$ was plotted to the Hall-Petch equation, and was found to only apply between 850°C to 950°C but beyond 950 °C, the relationship did not hold.

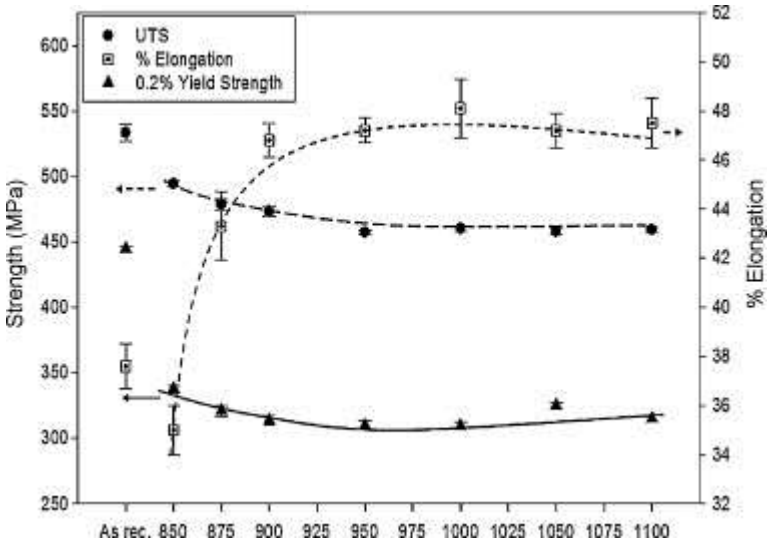

Fig. 7. Effect of annealing temperature at 850 °C and above on the tensile strength and elongation.

3.3 Effect of heat treatment on the Charpy impact energy and DBTT

CIE values at various testing temperatures on the heat treated specimens are shown in Fig. 8. Quenching from 850°C exhibits a maximum toughness of about 60J at 25°C and a Ductile-to-Brittle Transition Temperature (DBTT) of about 5°C at about 30J. Annealing at 950°C, however, resulted in the DBTT to rise to 40°C while all these specimens fractured in a brittle manner, due to a large grain size. On the other hand, the upper shelf energy for the specimens annealed at 950°C was found to be much higher, averaging about 90J.

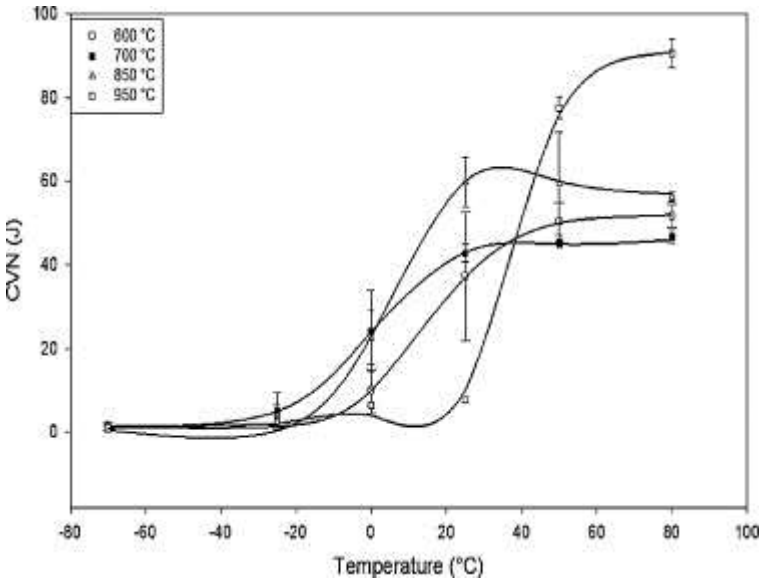

Fig. 8. Charpy impact energy as a function of the test temperature from specimens that were annealed at four different temperatures, both within and outside the Laves phase formation region.

The grain size after annealing varied from 22 to 60μm as the temperature was increased from 850 to 950°C (see Fig. 5). The DBTT in Fig. 8 rose with increasing grain size in both sets of specimens, but the upper shelf energy seems to be independent of the grain size, most likely caused by the presence of some Laves phase still present at the grain boundaries after annealing at 850°C (see Fig. 6(a)), thereby lowering the shelf energy to about 60J compared to the 90J after annealing at 950°C.

3.4 Effect of cooling rate on the room temperature Charpy impact energy

The effect of linear cooling rate on the room temperature impact toughness of the steel after annealing at 850°C and 950°C, respectively, is shown in Fig. 9. This simulated the effect of the post-hot rolling cooling rate on the final grain size and the precipitation of Laves phase and hence their impact on the CIE. Rapid cooling from 850°C gives higher impact energy than after cooling from 950°C, caused initially by a

difference in grain size. This is observed after cooling rates of 50°C/s, where there was a difference of 34J in the upper shelf energy between the two respective specimens; see Fig. 9, results that are comparable to those in Fig. 3. Note furthermore, that the impact strength after cooling from 950°C is only marginally affected by the cooling rate while this is not so after cooling from 850°C where faster cooling results in smaller volumes of Laves phase forming and hence in higher impact strengths. This is significant as it proves that the embrittling effects of a large grain size introduced by cooling from 950°C, overrides any further embrittlement by Laves phase caused by slow cooling.

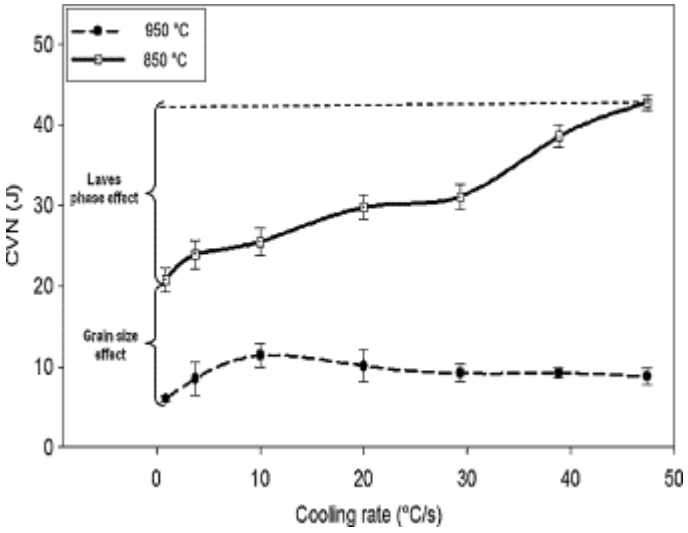

Fig. 9. Effect of linear cooling rate in °C/s on the room temperature impact toughness of the specimens that were cooled from 850 and 950 °C, respectively.

4 Discussion

4.1 Types of precipitates found in type AISI 441

The isopleth diagram for the phases that were expected to be stable and at equilibrium over a wide range of carbon content for this composition of the steel is shown in Fig. 1(b) of which the presence of the main constituent of Laves phase plus smaller amounts of (Ti,Nb)(C,N) were confirmed by XRD from the electrolytically extracted second phases. Angular carbo-nitrides of titanium and niobium observed here by both SEM and TEM, were also found to be randomly dispersed throughout the structure and these lower the melting point of the steel [15]. Excess niobium is taken into solid solution during high temperature annealing and is re-precipitated as very fine particles of the Laves phase (Fe_2Nb) upon either slow cooling or upon holding at intermediate temperatures of 600 to 950°C [16], leading to improved elevated temperature strength [17,18].

Although Thermo-Calc® calculations show the presence of the sigma phase as an equilibrium phase, others have indicated that this phase does not form in this type of alloy and none was found here. Sigma phase precipitates in high chromium ferritic stainless steels but only after very long periods at high service temperatures [19-21].

The solvus temperature for each phase in this alloy is composition dependent, i.e. for the Laves phase in this composition of steel it was calculated by Thermo-Calc® as 825°C but in practice in Fig.1 it was found to be about 875°C. A more detailed analysis of the kinetics of nucleation of the Laves and other second phases by XRD on electrolytically extracted precipitates in this and other similar Nb-containing ferritic stainless steels will be reported elsewhere [10].

4.2 Embrittlement by the Laves phase

From Fig. 3, the Charpy impact values indicate decreasing embrittlement with increasing annealing temperature up to 850°C through a decreasing volume fraction of Laves phase (see Fig. 1). In a Ti and Nb stabilised low C, N – 19%Cr – 2%Mo stainless steel Sawatani et al [17] observed that an increase in volume fraction of Laves phase embrittled this steel significantly, but the authors did not make any detailed analysis of the reasons for this. Grubb et al. [22] have suggested that embrittlement arises from the flow stress increase associated with α' – precipitation (i.e. 475°C embrittlement) and that this can be readily understood using the approach of Cottrell [23,24], which provides a useful basis for understanding the micromechanics of brittle fracture even though the model does not encompass all the practical modes of crack initiation. Ferritic stainless steels generally display a substantial increase in lattice friction stress upon rapid cooling, which leads to an increase in the DBTT, in accordance with Cottrell that predicted brittle fracture with grain size as a variable, will occur when:

$$\sigma_y k_y d^{1/2} = k_y^2 + \sigma_0 k_y d^{1/2} > C_1 G_M \gamma \qquad [1]$$

where σ_y is the yield strength, k_y is the Hall – Petch slope, d is the grain size, σ_0 is the lattice friction stress, G_M is the shear modulus, γ is the effective surface energy of an implied crack and C_1 is a constant. Generally, the toughness of ferritic steels can be assessed by the DBTT, or a temperature below which Equation 1 appears to be satisfied by the flow stress equalling the fracture stress, i.e. brittle fracture without any significant plastic yielding. The satisfaction of Equation 1 with decreasing temperature is associated with the tendency for the flow stress to increase with decreasing temperature. High strain rates and constraints to plastic flow at the root of a notch raise the flow stress and this lowers the value of

C_1, thus promoting satisfaction for Equation 1. According to the Cottrell model this may be explained by the locking of dislocations by interstitials in bcc materials that cause the flow stress to increase. However, the solubility level of the interstitials carbon and nitrogen in ferritic stainless steel is sufficiently low that it is rarely possible to distinguish between solute embrittling effects and the effect of second-phase precipitates.

The precipitates, in fact, become more important than the solute when the amount of interstitial elements significantly exceeds the solubility limit, and this serves to increase the DBTT still further. This embrittling effect is closely linked to the number and size of precipitates formed on the grain boundaries. Thick precipitate films act as strong barriers to slip propagation across the grain boundaries and raise k_y (see Fig. 10**.** In this case, an approach of Smith [25] can be used for growth controlled cleavage fracture that incorporates brittle precipitates on grain boundaries. Here a Laves phase particle of width C_o at the grain boundary is cracked by the dislocation pile – up of length d, which may be related to the grain size itself through the availability of the number of nucleation sites on grain boundaries. The fracture stress is predicted to be the effective shear stress, and it may be analysed in a manner similar to that for the Cottrell model to obtain a failure criterion in the absence of plastic flow:

$$\sigma_f > \left[\frac{4E\gamma_f}{\pi(1-\nu^2)C_o} \right]^{\frac{1}{2}} \qquad [2]$$

where E is Young's modulus, σ_f is the fracture stress; γ_f is the effective surface energy of the ferrite grain to the Laves particle, ν is Poisson's ratio, and C_o is the grain boundary Laves phase's thickness. This model indicates that coarser Laves particles with a higher value of C_o give rise to lower fracture stresses, and also predict that σ_f is independent of the grain size. However, in practice a fine grain size is associated with thinner particles due to a higher nucleation rate upon forming the particles, and the value of σ_f is then expected to be higher. Grain boundary Laves phase precipitation can be suppressed by quenching from above the solution temperature when the interstitial content is low. However, any fine intergranular precipitation may also increase the DBTT, as was actually found at 600°C in Fig.8, by increasing the lattice friction stress (σ_o). This model appears to explain at least qualitatively the cause of the embrittlement associated with the Laves phase in type AISI 441 steel.

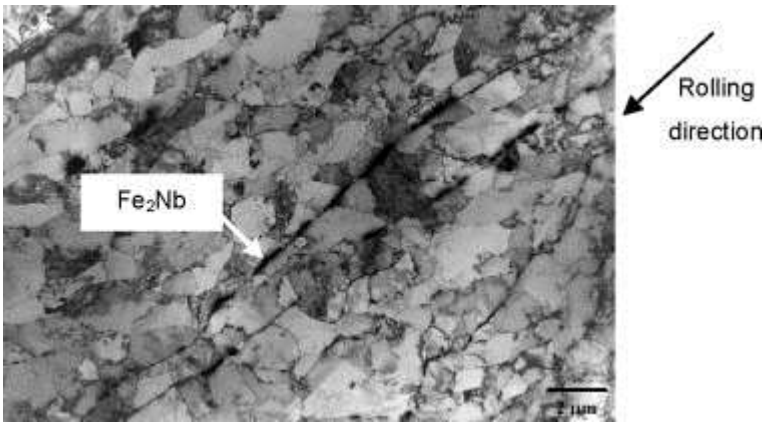

Fig. 10. TEM micrograph showing the presence of the fine Laves precipitates on the subgrain boundaries within the rolling bands of the specimen that had been annealed at 750 °C.

Sim et al. [5] have shown on a Nb stabilised ferritic stainless steel, that the high temperature strength decreases with increasing ageing time at temperatures between 600 and 950°C, mainly due to the loss of solid solution hardening as the Nb is transferred from the matrix into the Laves phase. They also observed that the rate of reduction in yield strength after annealing at 700°C, varied linearly with the Nb content in solid solution. They concluded that during ageing at 700°C, Nb(C,N) and Fe_3Nb_3C decrease the high temperature strength slowly while the precipitation of the Fe_2Nb Laves phase at 700°C decreases the high temperature strength more abruptly, probably because of the *Lifshitz-Slyosov-Wagner* (LSW) quasi-equilibrium coarsening rate of the Laves phase that appears to be much faster than that of Nb(C,N). This was believed by Sim et al [5] to be due to the incoherent but higher energy interface between the Fe_2Nb and the matrix than with the Nb(C,N). Coarse grain boundary Fe_2Nb precipitates are, therefore, detrimental to the high temperature strength of type AISI 441.

Other researchers on ferritic stainless steels have shown that the tensile strength increases with annealing temperature above 1000°C whilst the percentage elongation decreases [17]. From this it can be postulated that as the annealing temperature increases the amount of niobium in solution also increases from dissolution of precipitates and this should increase the yield strength from solid solution hardening. In the present work the same was not observed since the tensile strength decreased with increasing solution treatment temperature (see Fig. 7), probably from grain coarsening. In a ferritic steel with composition Fe–10at.% Cr–Nb with 0.5–5at.%Nb, Yamamoto et al. [18] observed that it is possible to strengthen a steel by Fe_2Nb Laves phase to give an excellent high temperature strength. They suggested that the strength is insensitive to Nb content, but an optimum concentration of about 1–1.5at.% Nb would

provide a proper volume fraction of the Laves phase to ensure good room temperature ductility. None of these authors, however, had attempted to make any correlation between the Laves phase volume fraction present and high strain rate or impact strength. It is well known that good strength and even good ductility values at slow strain rate testing without any sign of brittleness does occur and the practicality of strengthening these alloys by Laves phase needs to be approached with caution.

Both fracture and yield strength depend on grain size, and refining the latter will result in an increase of these strengths. According to Cottrell, the embrittlement from an increased grain size becomes effective when the flow stress practically equals the fracture stress with very little measurable plastic strain. In this case, that will be at 950°C where there is no grain boundary Laves phase present. From Fig. 5, the grain size increase between 950 and 1000°C is about 60%. From Equation 1 and by increasing the grain size, both the fracture stress and the flow stress will be decreased, and this will shift the DBTT upwards as found here. In work by Kinoshita [26] on 18Cr-2Mo and 26Cr–4Mo steels, no significant grain size dependence of the DBTT was found where the grain size was varied through strain annealing. However, many other authors have reported such a relationship as was also found here [22-24]. Where there are grain boundary precipitates present below 850°C, the Laves phase will lower the cleavage fracture stress. A crack nucleus is then formed by the separation of the particle–matrix interface, and this interfacial crack initiates transgranular fracture, but that has not been observed to cause grain separation.

When the specimens are slowly cooled from annealing above the Laves phase solvus temperature, precipitation of the Laves phase occurs during cooling. Steels embrittled from such a treatment behave similarly to those treated below the solvus temperature [25]. This points to the usefulness of constructing a (time – temperature – precipitation) *TTP* diagram for Laves phase formation and such a curve was determined experimentally in this steel and will be reported elsewhere [10]. Heat treatments that accelerate the precipitation of Laves phase (that is, below 900°C) decrease the resistance to crack initiation significantly during dynamic loading. The volume fraction of the Laves phase, particularly on the sub- and grain boundaries, plays a significant role in affecting both the DBTT and the upper-shelf energy and the degree of embrittlement should increase as the volume fraction increases at lower annealing temperatures (see Fig. 1) according to the Smith model of embrittlement by grain boundary phases in ferritic steels. The width C_o (in Equation 2) of the embrittling second phase is related to the volume fraction V_v of the Laves phase but also to the grain size, the latter through the grain boundary nucleation site concentration with a larger sub- and grain size leading to a thicker C_o through less available nucleation sites. Both a higher volume fraction as well as a larger sub- and grain size will then decrease

the effective fracture stress through a higher value of C_o. This was found in Fig. 3 with annealing temperatures decreasing from 850 to 600°C, raising the volume or weight fraction of the Laves phase (see Fig. 1). Other authors as well as from this study to be published elsewhere, have shown that there is an optimum annealing temperature at which the quantity of the Laves phase Fe_2Nb reaches a maximum, and this temperature depends critically on the Nb content in the steel [4,6], according to a relevant *TTP* diagram [10]. In the current work, therefore, the remaining quantity of Laves phase on grain boundaries at 850°C could have contributed to a reduced upper shelf energy than that found at 950°C where no Laves phase was present any more.

On specimens annealed at 600, 700 and 850°C, Fig.1 showed that the equilibrated weight fraction of the Laves phase at 600°C was about 0.92%wt, at 700°C about 0.67%wt, and with about 0.14wt% present at 850°C. In work to be reported elsewhere on the kinetics of the Laves phase formation, it was observed that the precipitation rate of the Laves phase is much higher at 700°C than at either 850 or 600°C, and this resulted in a double nose *TTP* curve [10]. At 700°C, therefore, after equal times at temperature, the volume fraction of the Laves phase was much higher than either at 850 or at 600°C, resulting in a lower upper shelf energy at 700°C than the specimen annealed at 600°C in Fig. 8.

At room temperature in Fig. 8, which falls within the ductile to brittle transitions but not at the same points for the two temperatures, annealing at 950°C is at the bottom of the transition while at 850°C it is in the middle. A direct comparison of the absolute room temperature impact values on the two curves is, therefore, not feasible as they fall within different parts of the transition curve. At 950°C the grain size effect is overwhelming (even more significant than the effect from the Laves phase) and the addition of Laves phase to an already brittle steel at slow cooling rates, brings in no measurable further embrittlement. Therefore, the full effect of Laves phase precipitation on the CIE is seen only after annealing at 850°C where the grain size after 30 minutes remained equal to that at lower temperatures. Therefore, annealing at 850°C produces a significant decrease in the CIE with slower cooling rates that allow Laves phase to form during cooling. Annealing at 950°C, however, shows only a slight increase in CIE after slow cooling of 10°C/s, and thereafter the toughness levels off with any further increase in cooling rate. Again, as the cooling rate from 950°C decreases the amount of Laves phase that forms must increase, but any further embrittlement from this is masked by the already severe embrittling grain size effect. These results largely agree with other researchers [17,24,26], with the cooling rate after solution

annealing having a pronounced influence on the impact energy transition of low interstitial ferritic stainless steels, with the lower cooling rates showing a higher DBTT.

4.3 Recrystallisation and grain growth

Although grain growth experienced in this alloy after annealing above 850°C is generally expected, the "sudden" significant increase in grain size by about 60% within the temperature region 950 to 1000°C cannot be readily explained by normal grain growth theories and needs some discussion. Firstly, "grain boundary particle unpinning by dissolution" through a Zener process [25,27] can be discounted as at 850°C where some last remnants of Laves phase were still found, the Zener pinning or retarding force may be relatively small, estimated at ~2 x 10^4 J/m^3 (i.e. small volume fraction and large radius of the Laves phase) and a condition will not easily be reached at this temperature where it effectively blocks full recrystallisation and subsequent grain growth. A number of authors [27,28] have proposed and observed an alternative process of "continuous recrystallisation" in aluminium alloys in which particles occupy mainly subgrain boundaries and these only become "released" after some coarsening of the particles, where after "full recrystallisation" appears to occur in a gradual process. That such a gradual process may have occurred also here is quite possible if the TEM microstructures after 850 and 900°C are compared in Figs. 6 (a) and (b). After annealing at 850°C subgrains are still present and heavily decorated by the last remnants of the Laves phase while at 900°C, the subgrain boundaries have completely disappeared and the grain boundaries are clean of any Laves or other phases. The effective rate of continuous recrystallisation is, therefore, determined by the rate of coarsening (which is accompanied by the rate of disappearance of the smaller particles), of the Laves phase particles. At 850°C, recovery has taken place but no recrystallisation while at 900°C full recrystallisation has taken place. This shows that at 850°C, the last remnants of the smaller Laves phase particles are still effective in locking subgrain boundaries but not at 900°C. The sudden increase in grain size between 950°C and 1000°C, therefore, was not due to an unpinning effect of the grain boundaries by the Laves phase, which had already disappeared between 850 and 900°C.

An alternative reasoning of "Nb solute drag of sub- and grain boundaries" may be considered in explaining this "sudden" 60% increase in grain size at annealing temperatures between 950 and 1000°C. The rate of movement v_b of a grain boundary is given by $v_b = p_d M_b$ where p_d is the driving force and M_b the boundary's mobility [29]. The quantitative theory of solute drag on a moving grain boundary was originally formulated by Lücke and Detert [29] and was later modified by Cahn [30] and then by Lücke and

Stüwe [31]. Since then, this theory has been further refined by several authors [32-34]. The equation proposed by Cahn on the rate of grain boundary movement as it is affected by solute drag is [35,36]:

$$\frac{p_d}{v_b} = \frac{1}{M_T} = \frac{1}{M_o} + \frac{\alpha X_s}{(1+\beta^2 v_b^2)} \qquad [4]$$

where p_d and v_b are defined as above, M_T is the overall mobility due to intrinsic plus solute drag, M_0 is the intrinsic grain boundary mobility in pure material, X_s is the atom concentration of solute in the bulk metal, α is a term related to the binding energy of solute to the grain boundary and β is a term related to the diffusion rate of the solute near the grain boundary. The product (αX_s) primarily governs the overall mobility M_T because $(1+\beta^2 v_b^2) > 1$, while if $(1+\beta^2 v_b^2) \gg 1$, then $M_T \approx M_0$ and no solute drag occurs and only intrinsic drag remains. The possibility that a fundamental change from "solute plus intrinsic drag by Nb atoms" (i.e. controlled by the overall mobility parameter M_T) to one of only "intrinsic drag" and now controlled only by the intrinsic mobility parameter M_0, may occur within the temperature range 950 to 1000°C in this alloy needs to be considered. The question, however, immediately then arises whether such a transition from "solute plus intrinsic drag" at lower temperatures to one of only "intrinsic drag" at about 950 to 1000°C would not rather be a gradual one than a "sudden" one? That such a "sudden" departure from solute plus intrinsic drag to only intrinsic drag occurs "suddenly" at critical concentrations of the solute or at critical temperatures, has indeed been found by some authors.

Firstly, such a sharp "break" in the effect of low level concentrations of Nb in solute drag on grain boundaries, was shown by Suehiro [32] in the theoretical analysis of small Nb-additions to iron where a two orders of magnitude sudden decrease in the grain boundary velocity v_b was predicted at 700ºC at a critical Nb concentration of 0.15%wt.

Secondly, the analysis by Le Gall and Jonas [35] of solute drag by sulphur atoms in pure nickel also showed that this transition from solute plus intrinsic drag to purely intrinsic mobility of a grain boundary is not a gradual one but occurs at a critical temperature that provides a "break" in the mobility versus inverse temperature relationship. Furthermore, this critical transition temperature was found to be highly dependent on the concentration of the "dragging" sulphur atoms in solution [36] and may in the steel 441, therefore, vary with different Nb concentrations in solution which, in turn, will be determined by the alloy content and/or by the heat treatments that have led to the Nb in solution. This mechanism remains currently as the only plausible mechanism for the accelerated grain growth between 950 and 1000°C and may be a useful avenue of further study.

5 Conclusions

The following may be concluded from this study:

- The plant-brittle as received AISI 441 steel showed a good room temperature impact toughness after being equilibrium annealed for 30 minutes at 850°C while below or above this heat treatment temperature the impact toughness decreases sharply. At temperatures above 850°C grain growth plays a dominant role in lowering the impact toughness, but at temperatures below 850°C, the low impact toughness was found to be associated with the precipitation of the intermetallic Laves phase on grain boundaries. The results of the effect of annealing temperature on the Laves phase precipitation largely agree with the prediction made by Thermo–Calc® as well as with the measured weight fractions on solution treated and isothermally annealed specimens, whereby an increase in Laves phase volume fraction resulted in lowering the room temperature impact toughness.

- The predicted Laves phase solvus temperature for this particular steel composition of 825°C, however, was found to rather be 875°C.

- The ductile–to–brittle transition temperature (DBTT) is dependent on both the grain size and the presence of Laves phase precipitates on grain boundaries, but the upper shelf energy is only dependent on the presence of the Laves phase precipitates.

- Cooling rate after solution annealing has a pronounced influence on the severity of the Laves phase embrittlement of the steel after annealing at 850°C. After cooling from 950°C with an already embrittled structure from grain growth, the introduction of Laves phase during slow cooling does not introduce measurable additional embrittlement. In steels of this type, the embrittlement caused by excessive grain growth is, therefore, overriding.
- Annealing at temperatures above 850°C in this alloy, generally expected grain growth was experienced, but with a “sudden” significant increase in grain size of about 60% within the temperature region 950 to 1000°C. As no grain boundary pinning was evident at these temperatures, it was postulated that the disappearance of Nb solute drag may be responsible for this “sudden release” of the grain boundaries, affecting the full recrystallisation and later grain growth of type AISI 441 steels at lower temperatures.

- Brittle-free 441 steels of this type, therefore, have a rather narrow temperature “window” of about 850°C coupled with a fast cooling rate thereafter in manufacture processing.
- It has been shown that an already plant-brittle processed steel type 441 could be recovered if solution treatment at about 850°C followed by rapid cooling were practically possible.

Acknowledgements

The authors would like to acknowledge the support of this work from Columbus Stainless, South Africa and the Department of Materials Science and Metallurgical Engineering of the University of Pretoria. The authors also kindly acknowledge permission to publish from both Columbus Stainless and the University of Pretoria.

Reference

1. N. Fujita, K. Ohmura, A. Yamamoto, *Mater. Sc. Eng.* A, 351 (2003) 272.
2. J-H. Schmitt, *Key Eng. Mater.,* 230 – 232 (2002) 17.
3. Y. Xiong-mi, J. Zhou-hua & L. Hua-bin, *J. Iron Steel Research, Int.,* 14 (2007) 24.
4. N. Fujita, K. Ohmura, M. Kikuchi, *Scripta Mater.,* 35 (1996) 705.
5. G. M. Sim, J. C. Ahn, S. C. Hong, *Mater. Sc. Eng.* A, 396 (2005) 159.
6. N. Fujita, H. K. D. H. Bhadeshia, M. Kikuchi, *Model. Simul. Mater. Sci. Eng.,* 12 (2004) 273.
7. D.G. Morris, M. A. Muñoz-Morris, C. Baudin, *Acta Mater.,* 52 (2004) 2827.
8. Columbus Stainless of South Africa, personal communication
9. J. C. Ahn, G. M. Sim, K. S. Lee, *Mater. Sci. Forum,* 475 – 479 (2005) 191.
10. M. P. Sello, W. E. Stumpf, to be published, also in the PhD Thesis of MP Sello (2009), University of Pretoria.
11. TCC^{TM} Thermo – Calc® Software User Guide Version Q
12. A. Bjärbo; *Scand. J. Metall.,* 35 (2003) 94.
13. A.J. Craven, K. He, L. A. J. Gravie, T. N. Baker, *Acta Mater.,* 48 (2000) 3857.
14. B. A. Senior, *Mater. Sc. Eng.* A, 119 (1989) L5 (letter)
15. W. Gordon, A. van Bennekom, *Mater. Sc. Eng.* A, 351 (2003) 126.
16. Technical Data Blue Sheet – Stainless Steel Type 441, AL 441HP Alloys, Allengheny Ludlum Corporation
17. T. Sawatani, S. Minomina, H. Morikawa, *Trans. ISIJ,* 22 (1982) 173.

18. K. Yamamoto, Y. Kimura, F-G. Wei, Y. Mishima, *Mater. Sc. Eng.* A, 329 – 331 (2002) 249.
19. G. Restrepo Garcé, J. Le Coze, J. L. Garin, R. L. Mannheim, *Scripta Mater.,* 50 (2004) 651.
20. T-H. Lee, C-S. Oh, C. G. Lee, S-J. Kim, S. Takaki, *Scripta Mater.,* 50 (2004) 1325.
21. V. Kuzucu, M. Aksoy, M. H. Korkut, *J. Mater. Proc. Technol.,* 82 (1998) 165.
22. J. F. Grubb, R. N. Wright, P. Farrar, Jr., In: *Toughness of ferritic stainless steel,* ASTM STP 706, R. A. Lula, Ed., American Society for Testing and Materials (1980) 56.
23. A. C. T. M. Van Zwieten, J. H. Bulloch, *Int. J. Press. Vessels & Piping* 56 (1993) 1.
24. R. N. Wright, *Toughness of ferritic stainless steel,* ASTM STP 706, R. A. Lula, Ed., American Society for Testing and Materials (1980) 202.
25. C. S. Smith, *Trans. Metall. Soc. of AIME* 175 (1948) 15.
26. N. Kinoshita, *Stainless Steel '84* (1984) 43
27. R. Higginson, P. Bate, *Acta Mater.,* 47(1999). 1079.
28. M.J. Jones, F.J. Humphreys, *Acta Mater.,* 51 (2003) 2149.
29. K. Lücke, K. Detert, *Acta Metall.,* 5 (1957) 628.
30. J. W. Cahn, *Acta Metall.,* 10 (1962) 178.
31. K. Lücke, H. P. Stüwe, *Acta Metall.,* 19 (1971) 1087.
32. M. Suehiro, *ISIJ Int.* 38 (1998) 547.
33. M. Suehiro, Z.-K. Lui, J. Ågren, *Acta Mater.*, 44 (1996) 4241.
34. M. Hillert, *Acta Mater*., 52 (2004) 5289.
35. R. Le Gall, J. J. Jonas, *Acta Mater.,* 47 (1999) 4365.
36. W. Stumpf, K. Banks, *Mater. Sc. Eng. A*, 418 (2006) 26.